

# The influence of the low-voltage capacitor dielectric material on the capacitive probe response in the nanosecond range

P. OSMOKROVIC<sup>a</sup>, A. VASIC<sup>b</sup>, M. VUJISIC<sup>a</sup>

<sup>a</sup>Faculty of Electrical Engineering, University of Belgrade, Bulevar Kralja Aleksandra 73, P.O.Box 3554, 11000 Belgrade, Serbia & Montenegro

<sup>b</sup>Faculty of Mechanical Engineering, University of Belgrade, Kraljice Marije 16, 11120 Belgrade, Serbia & Montenegro

This paper investigates the influence of the low-voltage capacitor dielectric material on the capacitive probe response in the nanosecond range. It was inferred which types of microscopic material structure, i.e. types of frequency characteristics of the material, would best suit the purpose. The capacitive probe with optimal characteristics was designed. An experimental system was formed, with the probe incorporated into the l-element of the pulse power generator (PPG). Measurements of the probe response in the nanosecond range were verified by numerical simulation. The use of materials with electronic polarization as low-voltage capacitor dielectrics confirmed the conclusions regarding their suitability for this purpose.

(Received December 22, 2005; accepted January 26, 2006)

**Keywords:** Pulsed power generator (PPG), Probe material (PM), Very fast transient (VFT)

## 1. Introduction

In the course of design, construction and exploitation of a pulsed power generator (PPG) it is necessary to determine the volume distribution of its internal transient electromagnetic field. Since this distribution is not unambiguously defined by the PPG geometry, it is necessary to design probes for VFT supervision. Compensated capacitive dividers, in combination with an analogue or digital oscilloscope, are used for VFT supervision at a PPG. In order to achieve minimal measurement uncertainty, all the elements of the probe must have characteristic response times much shorter than the duration of the measured phenomena, considering basic user requirements [1], [2], [3].

## 2. The precise capacitive probe

### 2.1 Working principles

The operating principle of the precise capacitive probe is that of a capacitive voltage divider (Fig. 1). The measured signal  $u_1(t)$  is applied to the high voltage capacitor  $C_1$ . The measuring signal  $u_2(t)$  is taken across the low-voltage capacitor  $C_2$  and led onto the recording apparatus.

Essential requirements for the reliable operation of the capacitive probe at the PPG (as well as of any capacitive voltage divider) are: 1) matching of the high- and low-voltage capacitors and 2) low-inductance probe design [4]. Matching of the high- and low-voltage capacitors refers to the transfer ratio  $n = C_1/C_2$  being independent of frequency. Low-inductance of the probe is achieved by the

appropriate design, which incorporates the radial form and minimal wiring length.

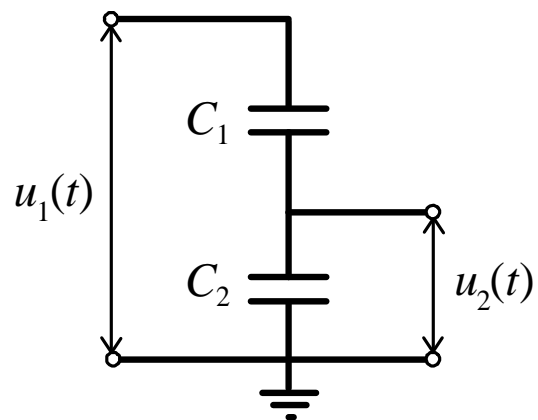


Fig. 1. Capacitive voltage divider.

### 2.2 High-voltage capacitor (probe sensor)

The principle scheme of the probe sensor is shown in Fig. 2. In an equivalent electrical scheme, the current  $i(t)$  which flows through the measuring circuit can be obtained by integrating the current density  $J(t)$  and the displacement current  $\partial D(t)/\partial t$  over the surface of the sensor  $A$ :

$$i(t) = \int_A \vec{J} d\vec{A} + \int_A \frac{\partial \vec{D}}{\partial t} d\vec{A} \quad (1)$$

In case of an infinitely conductive sensor surface and of a homogenous electrical field at the sensor, the expression (1) can be transformed into:

$$i(t) = \left[ \sigma E(t) + \varepsilon \frac{\partial E(t)}{\partial t} \right] A \quad (2)$$

where  $\sigma$  is the electrical conductivity and  $\varepsilon$  the dielectric constant.

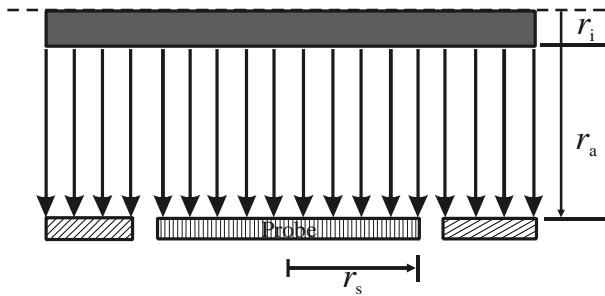


Fig. 2. The principle scheme of the probe sensor.

In the majority of cases the load of the sensor can be represented by a capacitor  $C$  (taking into account controlled and stray capacitance) and a parallel resistor  $R$  (comprising the compensation resistor and the resistance of connectors). Equation describing the corresponding equivalent electrical circuit is:

$$\left( \frac{1}{R} + C \frac{\partial}{\partial t} \right) u_1(t) = i(t) \quad (3)$$

which combined with (2) gives:

$$u_1(t) + RC \frac{\partial u_1(t)}{\partial t} = \left[ E(t) + \frac{\varepsilon}{\sigma} \frac{\partial E(t)}{\partial t} \right] \sigma AR \quad (4)$$

where  $u_1(t)$  is the measured voltage signal. When  $\varepsilon/\sigma = RC$ , equation (4) becomes:

$$u_1(t) = \frac{\varepsilon}{C} AE(t) \quad (5)$$

The condition of time constant equivalence  $\varepsilon/\sigma = RC$  is analogous to the compensation condition of an ohmic-capacitive voltage divider. According to expression (5) the response of the compensated sensor is proportional to the values of the electric field and the sensor surface.

When the transition time of the measured signal's progressive wave front along the sensor's spatial dimensions is not negligible compared to the measured

signal rise time, the measured voltage  $u_1(t)$  will be delayed from the measured signal  $E(t)$  and deviations from expression (5) arise. For the allowed measurement uncertainty of 2% the transition time of the progressive wave over the sensor surface should not exceed 1/5 of the measured signal rise time.

Apart from this most prominent effect, sensor dimensions will affect the response speed by two additional mechanisms: 1) oscillations and multiple reflections of the measured signal's progressive wave along the sensor axis, and 2) oscillations in the azimuthal direction of the cylindrical sensor [5,6,7].

### 2.3 Low-voltage capacitor

In high-voltage engineering the low-voltage capacitor of the capacitive divider is considerably larger than the high-voltage capacitor. The limiting factor in designing the low-voltage capacitor is the high frequency transfer characteristic of the divider. It is determined by the first resonant frequency of a weakly attenuated resonant circuit consisting of the parasitic inductance (inductance of the leads, capacitor plates, contacts, etc.) and the low-voltage capacitor of the divider:

$$f = \frac{1}{\sqrt{2\pi LC}} \quad (6)$$

This frequency is also called the upper frequency limit. The construction of the large capacitance low-voltage capacitor with the satisfactory high frequency transfer characteristics requires complex problems to be solved, particularly with regard to its design and the proper material choice.

### 2.4 Matching of the high- and low-voltage capacitors

The measuring probe should enable satisfactory transfer functions in voltage and frequency domains. The smallest distortion within the voltage domain will be obtained when the high-voltage capacitor and the low-voltage capacitor are gas capacitors [7]. This condition is not fulfilled in the probe presented here. For the probe to be used at a PPG, the high-voltage capacitor dielectric material should be deionized water. In order to achieve better linearity of characteristics, a gas high-voltage capacitor was used in this paper (with no electrodynamic phenomena, no partial discharges), equal to the probe sensor capacitance. The low-voltage capacitor was chosen to be a continual capacitor with a solid dielectric.

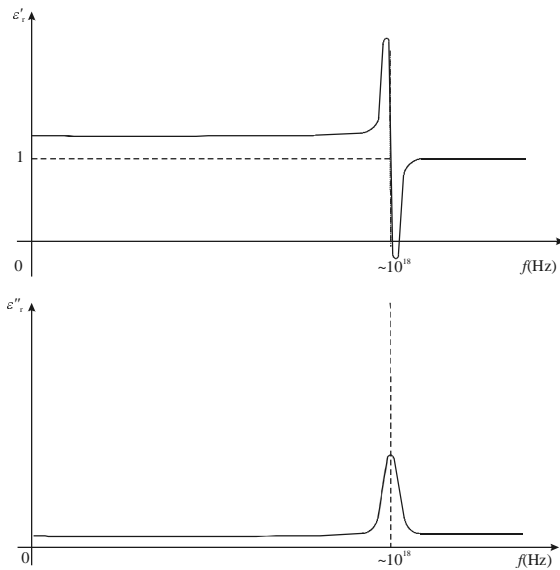


Fig. 3. Frequency dependence of the relative dielectric constant  $\epsilon_r(f)$  for a dielectric with only electronic polarization.

In such a case, for the transfer ratio to be independent of frequency, the low-voltage capacitor dielectric material has to have only electronic polarization. Materials of this kind show a simple frequency dependence of the complex relative dielectric constant  $\epsilon_r = \epsilon_r' - j\epsilon_r''$  (Fig. 3). Utilization of materials with electronic polarization provides a constant transfer ratio up to frequencies of  $10^{18}$  Hz, which by far surpasses the needs of the measurements in the nanosecond range (1 GHz). This could not have been achieved with materials having other types of polarization (interlayer, orientational, ionic), due to the intricate frequency dependence of their complex relative dielectric constant (Fig. 4).

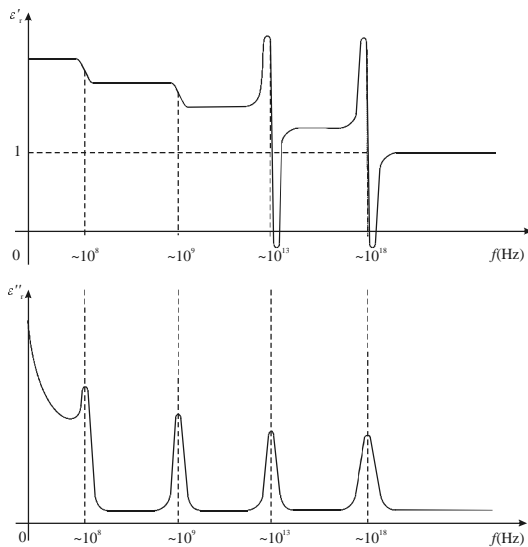


Fig. 4. Frequency dependence of the relative dielectric constant  $\epsilon_r(f)$  for a dielectric with all types of polarization.

### 3. The precise capacitive probe construction

#### 3.1 Construction of the high-voltage capacitor

The solution for the high-voltage capacitor construction should be adjusted to the measuring point. The expression for the electrical field in coaxial geometry can be used for calculating the high-voltage capacitance:

$$C_1 = \epsilon\pi r_s \frac{\arcsin(r_s / r_a)}{\ln(r_s / r_a)} \quad (7)$$

where  $\epsilon$  is the dielectric constant of the material,  $r_s$  is the probe sensor radius,  $r_i$  is the external radius of the lead, and  $r_a$  is the distance between the sensor and the lead axis (as designated in Fig. 2).

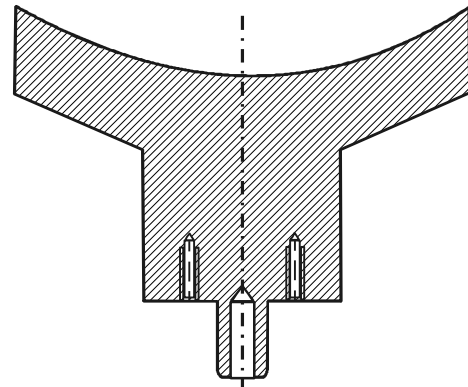


Fig. 5. Cross section of the probe sensor with a 90 mm diameter.

For the purpose of this paper the probe sensor with a 90 mm diameter was used. The corresponding capacitance of the high-voltage capacitor was 0.37 pF. Cross section of the sensor is shown in Fig. 5. The sensor is dimensioned in a way to ensure the recording of impulses with 1 ns rise time with measurement uncertainty below 3 %, providing a satisfactory response in the considered VFT frequency range.

#### 3.2 Construction of the low-voltage capacitor

One common disadvantage of low-voltage capacitors is a relatively high stray inductance introduced by long conductive paths. As a result, significant oscillations and reflections occur in the measuring system. To avoid such effects, the high- and low-voltage capacitors are integrated, and the adjustable resistor is given a continual conical structure (Fig. 6). Such a probe has the low-voltage capacitor next to the sensor itself. The conical form of the adjustable resistor enables a continuous transition to the measuring cable with corresponding wave impedance. When designing the cone, the condition to be fulfilled is:

$$Z_c = \frac{60}{\sqrt{\epsilon_r}} \ln \frac{\tan(\theta_2/2)}{\tan(\theta_1/2)} \quad (8)$$

where  $\theta_1$  is the angle of the output section of the probe sensor,  $\theta_2$  is the angle of the conical casing and  $Z_c$  is the cable wave impedance for which the adjustment is made.

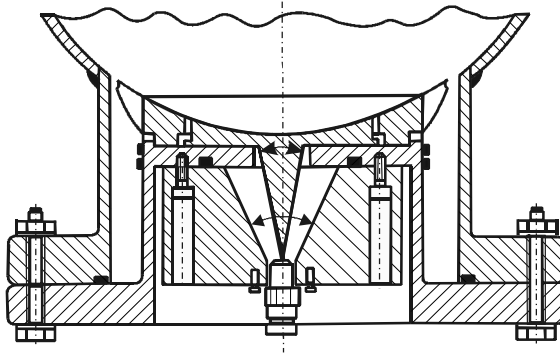


Fig. 6. The construction of the capacitive probe with the continual 50  $\Omega$  resistor.

Capacitance of the low-voltage capacitor was 1.95  $\mu\text{F}$ . Metalized polymer foils (30  $\mu\text{m}$  thick) were used as the low-voltage capacitor dielectric. Polymer materials used included: polyester, teflon, hostafan, polypropylene, polyvinylchloride, polytetrafluoretilene, polyamid, and polyurethane. All these materials fulfill the established condition for matching the high- and low-voltage capacitors.

#### 4. Verification by computer modeling

The measuring system for VFT supervision could not have been tested using methods adopted for usual measuring systems, due to the specific nature of the measurement and the position of the measuring point. It was necessary to construct an appropriate experimental setting and apply a combined computer / experimental procedure. A method for testing the measuring system response and checking the characteristics of the experimental setting transfer impedance was established by injecting a measured voltage wave into the I-element (test object) with an integrated measuring probe. A highly precise prediction of the measuring system response to the measured wave was obtained by computer modeling, using verified programs such as EMTP-ATP. The measured wave used for testing is represented by the function:

$$f(t) = k(e^t - e^{-t}) \quad (9)$$

for the given parameter values. Responses obtained by computer modeling were then compared to experimentally obtained ones [8,9,10].

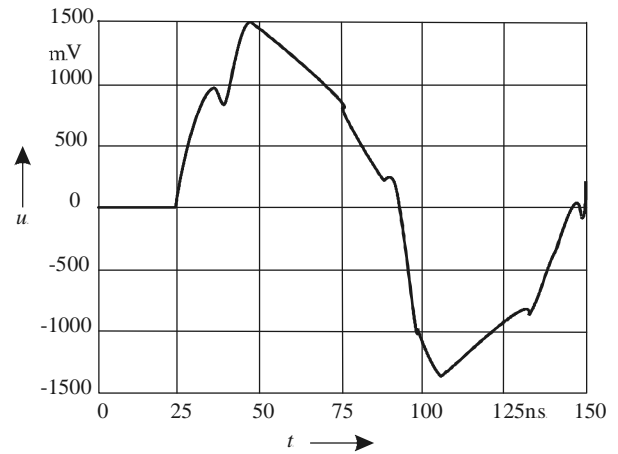


Fig. 7. Measuring system response obtained by computer modeling.

The measuring system response obtained from the computer is presented in Fig. 7 and the corresponding measuring system response obtained experimentally is shown in Fig. 8.

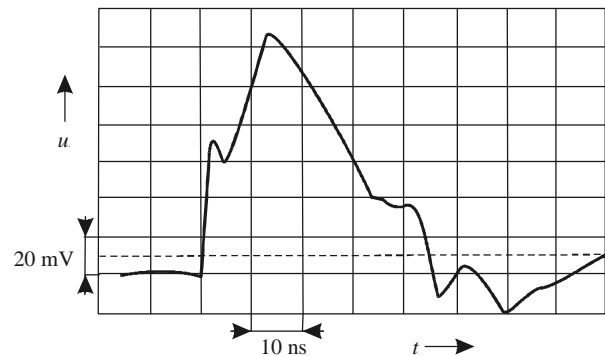


Fig. 8. Oscillogram of the measuring system response obtained experimentally.

When these responses are compared, certain differences can be noticed. These differences most probably result from the following: 1) The measured wave generated by the computer may deviate from the real measured wave; 2) The computer modeling of the PPG may deviate from the real situation, since the PPG model does not include impedance, while in reality certain impedance exists; 3) There is a difference between the time needed for the reflected or the refracted wave to return to the measuring point and the characteristic time of the measured wave; 4) The value of the concentrated capacitance (representing the disc at the end of the I-element used as the test object) is not accurately known. The largest effect is that of the PPG modeling.

It can be inferred that there is a very high correlation between responses obtained from the computer and experimentally obtained ones, up to those coordinates which are immediately behind the doubled wave.

Therefore, the experimental setting can be used for the verification of the measuring system for VFT supervision.

## 5. Results of the measuring system testing

The response of the measuring system with the integrated probe is presented in Fig. 9. The response time increases of the measuring system, obtained from the corresponding oscillograms are presented in Table 1.

Table 1. Response times of the measuring system.

MATERIAL	t [ns] - probe 75 $\Omega$	t [ns] - probe 50 $\Omega$
Polyester	5.22	5.40
Teflon	5.30	5.40
Hostafan	5.30	5.40
Polypropylene	5.30	5.40
Polyvinilechloride	5.32	5.42
Polytetrafluoretilene	5.32	5.42
Polyamid	5.32	5.42
Polyurethane	5.32	5.42

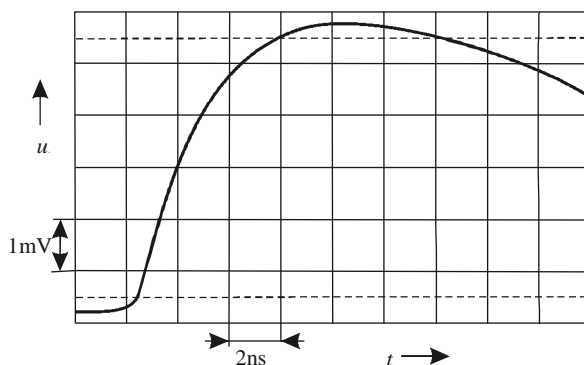


Fig. 9. Oscillogram of the measuring system response on the PPG output voltage wave with 5/50 ns form (end-resistors of 50  $\Omega$ ; polyester dielectric material).

On the basis of the results presented in Fig. 9 and Table 1, it can be concluded that the designed measuring system has satisfactory characteristics for VFT measurements at a PPG. The upper frequency limit with the integrated probe could not be determined precisely in

some cases, since the response of the system was identical to the measured wave. All of the tested materials are satisfactory for the implementation as low-voltage capacitor dielectrics. Response time differences are within the range of the measurement uncertainty.

## 6. Conclusion

This paper analyzes the connection between microscopic characteristics of the low-voltage capacitor dielectric material and the response of the capacitive probe for VFT supervision at a PPG. It is pointed out that the best results may be expected by using materials with electronic polarization of molecules. This conclusion has been experimentally verified. The obtained results show that a capacitive probe, with an optimal design and with a polymer low-voltage capacitor dielectric, transfers the measuring signal in the nanosecond range without distortion.

## References

- [1] J. Meppelink, K. Feser, W. Pfaff, Proc. IEEE-PES Winter Meeting, New York, 1988, pp. 1141.
- [2] W. Boeck, R. Witzmann, Proc. 5 th ISH, Braunschweig, 1987, pp. 12.01.
- [3] R. W. P. King, D. J. Bleyer, IEEE Transaction on Electromagnetic Compatibility, pp. 32-39, 1988.
- [4] A. Kuchler, Erfassung transienter elektromagnetischer Feldverteilungen mit konzentrierten und raumlich ausgedehnten Sensoren, Düsseldorf, Germany: VDI Verlag, 1987.
- [5] K. W. Struve, M. L. Horry, R. B. Spielman, Proc. PPC.
- [6] M. S. Di Capua, Proc. IEEE/IMTC, Tampa, Italy, 1985.
- [7] K. Giebig, P. Osmokrović, A. Schwab, Proc. 4th ISH, Athens, Greece, 1983, pp. 52.04.
- [8] P. Osmokrović, IEEE Trans. Power Delivery **4**, 2095 (1989).
- [9] P. Osmokrović, D. Petković, O. Marković, N. Kartalović, Đ. Vukić, ETEP **24**, 165 (1997).
- [10] P. Osmokrović, D. Petković, O. Marković, IEEE Trans. Instrumentation and Measurement **46**, 36 (1997).